Molecular Phylogenetics and Evolution 61 (2011) 933–943

Contents lists available at SciVerse ScienceDirect

Molecular Phylogenetics and Evolution

journal homepage: www.elsevier.com/locate/ympev

A multilocus phylogeny of the desmid genus *Micrasterias* (Streptophyta): Evidence for the accelerated rate of morphological evolution in protists

Pavel Škaloud *, Katarína Nemjová, Jana Veselá, Kateřina Černá, Jiří Neustupa

Department of Botany, Faculty of Science, Charles University in Prague, Benátská 2, Praha 2 CZ-12801, Czech Republic

ARTICLE INFO

Article history:
Received 9 June 2011
Revised 4 August 2011
Accepted 21 August 2011
Available online 3 September 2011

Keywords:
Biogeography
Evolution
Micrasterias
Morphology
Phylogeny
Protists

ABSTRACT

Micrasterias, the name of which is derived from the Greek for 'little star', comprises possibly the most spectacularly shaped desmids (Desmidiales, Streptophyta). Presently, the genus *Micrasterias* includes about 60 traditional species, the majority of which were described in the early 19th century. We used a comprehensive multigene dataset (including SSU rDNA, *psa*A, and *cox*III loci) of 34 *Micrasterias* taxa to assess the relationships between individual morphological species. The resulting phylogeny was used to assess the patterns characterizing the morphological evolution of this genus. The phylogenetic analysis led to the recognition of eight well-resolved lineages that could be characterized by selected morphological features. Apart from the members of *Micrasterias*, three species belonged to different traditional desmid genera (*Cosmarium*, *Staurodesmus*, and *Triploceras*) and were inferred to be nested within the genus. Morphological comparisons of these species with their relatives revealed an accelerated rate of morphological evolution. Mapping morphological diversification of the genus on the phylogenetic tree revealed profound differences in the phylogenetic signal of selected phenotypic features. Whereas the branching pattern of the cells clearly correlated with the phylogeny, cell complexity possibly reflected rather their adaptive morphological responses to environmental conditions. Finally, ancestral reconstruction of distribution patterns indicated potential origin of the genus in North America, with additional speciation events occurring in the Indo-Malaysian region.

1. Introduction

Microbial eukaryotes often have few morphological characters, thus their morphological species identification is very difficult. Contrary to the situation for macroorganisms, the simple morphology of microorganisms often leads to convergent morphological evolution across different phylogenetic lineages. For example, the species of morphologically defined coccoid genus *Chlorella* were revealed to be dispersed over two classes of chlorophytes, the Chlorophyceae and the Trebouxiophyceae (Huss et al., 1999). Indeed, according to the present knowledge, the traditionally conceived genus *Chlorella* forms at least nine independent lineages corresponding to different genera (An et al., 1999; Darienko et al., 2010; Huss et al., 1999; Krienitz et al., 2004; Neustupa et al., 2009b).

Recently, incongruence between morphological and genetic similarities was also demonstrated for conjugating green algae (Zygnematophyceae), the green algal group that is more closely related to embryophyte land plants than to other green algae (Lewis and McCourt, 2004). Within their most species-rich family Desmidiaceae (desmids), those forms exhibiting small cell sizes and simple morphologies (e.g., the genera *Cosmarium* and *Staurodesmus*) were found to have arisen independently during evolution (Gontcharov, 2008; Gontcharov and Melkonian, 2008; Hall et al., 2008). As in the genus *Chlorella*, polyphyly of these morphotypes has been caused by convergent morphological evolution towards the most simple cell shapes. However, phylogenetic studies also demonstrated the polyphyletic/paraphyletic nature of morphologically more complex genera, including one of the most prominent taxon, the genus *Micrasterias* (Gontcharov, 2008; Gontcharov and Melkonian, 2008; Gontcharov et al., 2003).

Micrasterias, the name of which is derived from the Greek for 'little star', comprises one of the most spectacularly shaped organisms within Desmidiaceae. Cells are flattened and disc-like, consisting of two identical, symmetrical compartments (semicells). Each semicell has one polar lobe and two lateral lobes. One of the most prominent morphological features of the genus is the repeated branching of lateral cell lobes (Fig. 1). Presence of the first to fourth order lobes has been considered to be one of the most important morphological taxonomic characters within the genus (Krieger, 1939; Prescott et al., 1977). Cells of several *Micrasterias* species belong to the largest desmid genera, reaching 400 μm in diameter. Such cell dimensions of several frequently occurring species (e.g., *Micrasterias rotata* and *Micrasterias thomasiana*) even allow their

* Corresponding author. Fax: +420 221 951 645.
E-mail address: skaloud@natur.cuni.cz (P. Škaloud).

1055-7903/$ - see front matter © 2011 Elsevier Inc. All rights reserved.
doi:10.1016/j.ympev.2011.08.018

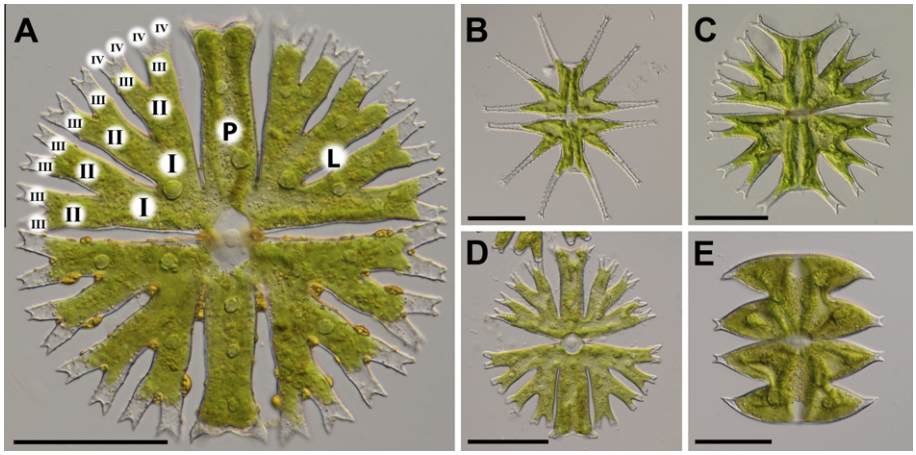

Fig. 1. Light micrographs of *Micrasterias*. (A) General morphology (*M. radiosa*). The cells are usually solitary, much compressed, with very deep median constriction (isthmus) dividing the cell into two semicells. Other shallow or deep incisions divide each semicell into a polar lobe (P) and two lateral lobes (L), each usually further subdivided. According to the degree of lobulation, the lateral lobes could be divided into the first (I), second (II), third (III) or fourth (IV) orders. The illustrated cell of *M. radiosa* is divided into the fourth order. (B) Cell with polar lobes divided into the first order (*M. hardyi*). (C) Cell with polar lobes divided into the second order (*M. furcata*). (D) Cell with polar lobes divided into the third order (*M. swainei*). (E) Cell with single, unbranched lobes (*M. laticeps*). Scale bar – 50 μm.

direct observation in natural habitats, where they could be detected as an assemblage of numerous little green discs. Due to their considerable cell sizes and spectacular shapes, *Micrasterias* species have attracted the attention of biologists for almost 200 years, since its description in the beginning of the 19th century (Agardh, 1827). The genus was widely used in various taxonomical, physiological, and morphogenetic studies, including artificial production of polyploid or enucleate cells (for reviews see Meindl, 1993 and Pickett-Heaps, 1975). Presently, the genus *Micrasterias* comprises about 60 species and several hundreds of subspecific taxa (Krieger, 1939; Růžička, 1981). Interestingly, the most of taxa were described already in the 19th century and only about 30% of them were added during the 20th century.

Considering the morphological peculiarity of *Micrasterias* species, it is hard to imagine that this cell shape pattern could have evolved independently several times during the evolution of zygnematophycean green algae. However, recent molecular phylogenetic studies attest to the fact that several morphologically distinct species (traditionally assigned to genera *Triploceras*, *Cosmarium*, and *Staurodesmus*) are nested within the phylogenetic lineage comprising *Micrasterias* taxa (Gontcharov, 2008; Gontcharov and Melkonian, 2008, 2011; Gontcharov et al., 2003; Hall et al., 2008; Neustupa et al., 2010). These molecular data indicated either independent origin of *Micrasterias* morphotype in unrelated taxa or existence of substantial morphological transformations during diversification of the genus *Micrasterias*, leading to the origin of morphologically different forms.

The principle aim of this paper was to trace evolutionary phenotypic transformations leading to the existence of morphologically different but genetically related species within the genus *Micrasterias*. Consequently, we aimed to (1) determine the phylogenetic position and closest relatives of morphologically anomalous species, by inferring a robust phylogeny of the genus, (2) define natural groups of related *Micrasterias* species, (3) assess which morphological traits are correlated with the evolutionary structure of the genus, and (4) estimate possible biogeographic origins of the genus by tracing the distribution patterns of individual *Micrasterias* species. We used a comprehensive multigene dataset (including nuclear, plastid, and mitochondrial markers) on 41 desmid strains to assess relationships among individual morphotypes, obtaining an insight into the patterns that have characterized the evolution of this genus.

2. Materials and methods

2.1. Origin and cultivation of strains, microscopic observations

Strains used in this study were obtained from five public culture collections: Sammlung von Conjugaten-Kulturen, University Hamburg (SVCK); Culture Collection of Algae, Charles University in Prague (CAUP); Culture Collection of Algae, University of Vienna (ASW), nowadays deposited in the Culture Collection of Algae at the University of Cologne (CCAC); Culture Collection of Algae, Georg-August University Göttingen (SAG); and Microbial Culture Collection, National Institute for Environmental Studies, Onogawa (NIES) (Supplementary Data 1). They were grown in 100-ml Erlenmeyer flasks in liquid oligotrophic medium used in the CAUP culture collection (Supplementary Data 2). Strains were maintained at a temperature of 15 °C, under an illumination of 5–15 μmol m^{-2} s^{-1} (cooling box Helkama C5G). All strains were observed under an Olympus BX51 light microscope (Olympus, Tokyo, Japan) to check their correct species identification. Microphotographs were taken with Olympus Z5060 digital micro-photographic equipment.

2.2. DNA extraction, polymerase chain reaction (PCR), and DNA sequencing

After centrifugation and mechanical disruption of cells by shaking in the presence of glass beads (0.5 mm in diameter, Sigma), the genomic DNA was extracted using the Invisorb Spin Plant Mini Kit (Invitek), following the manufacturer's instructions. Three molecular markers were amplified by PCR: nuclear SSU rDNA, chloroplast *psa*A, and mitochondrial *cox*III. PCR amplification of SSU rDNA was performed as described in Neustupa and Škaloud (2007). Two other genes were amplified as described in Hall et al. (2008), using either a XP thermal cycler (Bioer) or a Touchgene gradient cycler (Techne). The PCR products were quantified on a 1% agarose gel stained with ethidium bromide and cleaned with the JetQuick PCR Purification Kit (Genomed), according to the manufacturer's protocol. The purified amplification products were sequenced using an Applied Biosystems (Seoul, Korea) automated sequencer (ABI 3730xl) at Macrogen Corp. in Seoul, Korea. Sequencing reads were assembled and edited using the SeqAssem programme (Hepperle, 2004).

Sequencing results of several *Micrasterias* species indicated the presence of several polymorphic sites in *cox*III locus when using the PCR primers published by Hall et al. (2008). The sequence heterogeneity within a single species was often higher than that between different species, suggesting an existence of paralogous genes. Therefore, new internal primers were designed to resolve this problem: COX-ZYG-F3 (5′-TTA CTG GAG GTG GCA CAC TT-3′) and COX-ZYG-R2 (5′-TCC ATG AAA TCC AGT AGC TAA G-3′).

2.3. Sequence alignment and model selection

Multiple alignments of the newly determined SSU rDNA, *psa*A, *cox*III, and other sequences selected from the DDBJ/EMBL/GenBank databases were built using MUSCLE (Edgar, 2004) and edited manually using MEGA 4 (Kumar et al., 2008). The alignment of SSU rDNA sequences was guided by the secondary structure model of the *Closterium* 18S rRNA (Denboh et al., 2001).

A suitable partitioning strategy and partition-specific substitution models were selected in a multi-step process (Verbruggen et al., 2010). Initially, a guide tree was obtained by carrying out a second-level ML search on the unpartitioned dataset with a HKY + Γ_8 model using TreeFinder (Jobb, 2008). Then, the dataset was divided by 12 different partitioning strategies (combining different levels of loci segmentation). Subsequently, Bayesian information criterion (BIC) calculations were performed for all 12 potential partitioning strategies, assuming the guide tree and HKY + Γ_8 model for each partition. The four best-scoring partitioning strategies (receiving lowest BIC scores) were retained for further analysis. In the next step, models of sequence evolution were selected for individual partitions using the BIC. For each partition present in the four retained partitioning strategies, 12 different nucleotide substitution models were evaluated (F81, HKY, GTR, and their combinations with Γ, I, and Γ + I). Finally, the partitioning strategies were re-evaluated using selected models for particular partitions. This BIC-based model selection procedure selected the following model with six partitions: (1) stem region of SSU rDNA (GTR + Γ), (2) loop region of SSU rDNA (GTR + Γ), (3) 1st and 2nd codon position of *psa*A (F81 + Γ), (4) 3rd codon position of *psa*A (GTR + Γ), (5) 1st and 2nd codon position of *cox*III (F81 + Γ), and (6) 3rd codon position of *cox*III (HKY).

2.4. Molecular data and phylogenetic analyses

The amount of phylogenetic signal vs. noise in different molecular markers was assessed by two approaches. First, we plotted the uncorrected against corrected distances determined with the respective model of sequence evolution estimated by the program MODELTEST version 3.06 (Posada and Crandall, 1998). The estimated models were: GTR + Γ + I for SSU rDNA, HKY + Γ + I for *psa*A, and GTR + G for *cox*III. Second, the phylogenetic signal present in the data partitions was estimated by maximum likelihood mapping (Strimmer and von Haeseler, 1997) using the TREEPUZZLE 5.2 program (Schmidt et al., 2002).

The phylogenetic tree was inferred by Bayesian inference (BI) using MrBayes version 3.1 (Ronquist and Huelsenbeck, 2003). The analysis was carried out on the partitioned dataset using the strategy selected in the multi-step process described above. For the stem region of SSU rDNA, the doublet model (a 16-state RNA stem substitution model) was selected (Schöniger and von Haeseler, 1994; Skaloud and Peksa, 2010). All parameters were unlinked among partitions. Two parallel Markov chain Monte Carlo (MCMC) runs were carried out for 3 million generations, each with one cold and three heated chains. Trees and parameters were sampled every 100 generations. Convergence of the two cold chains was checked and burn-in was determined using the 'sump' command. Bootstrap analyses were performed by maximum likelihood (ML) and weighted parsimony (wMP) criteria using TreeFinder and PAUP* version 4.0b10 (Swofford, 2002), respectively. ML bootstrap values were obtained by running ML bootstrap analysis (1000 replications) under the partitioned dataset. The wMP bootstrapping (1000 replications) was performed using heuristic searches with 100 random sequence addition replicates; tree bisection reconnection swapping, random addition of sequences (the number limited to 10,000 for each replicate), and gap characters were treated as missing data. The weight to the characters has been assigned using the rescaled consistency index, in a scale from 0 to 1000. New weights were based on the mean of the fit values for each character over all of the trees in memory.

Congruence between the single-locus phylogenies was inferred by inspecting posterior probability values $\geqslant$0.95 resulting from separate Bayesian phylogenetic analyses of the SSU rDNA, *psa*A, and *cox*III datasets (Mason-Gamer and Kellogg, 1996), using the partitioning strategy as described above.

2.5. Character evolution

The evolution of selected morphological characters and geographic origin was traced along the tree using several ancestral state reconstruction techniques. Data on the average cell length and lobe division of particular *Micrasterias* species were obtained from Krieger (1939). Data on geographic distribution of individual species were obtained by an exhaustive analysis of available taxonomic monographs and floristic papers (see Supplementary Data 3).

Shape complexity analysis was based on generalized Procrustes superimposition analysis (GPA) of 144 landmarks placed along cellular outlines (Černá and Neustupa, 2010; Neustupa et al., 2008). The superimposition standardizes the size of the object and optimizes the rotation and translation so that the distances between corresponding landmarks are minimized (Zelditch et al., 2004). Then, complexity was estimated as the sum of Euclidean distances between adjacent landmarks along the outline in the size-standardized configurations (Neustupa et al., 2009a). The ancestral states of continuous data (cell length and cell complexity) were calculated in the program R, v2.9.2 (The R Foundation for Statistical Computing 2009, http://www.r-project.org/) using the Ape and Geiger packages (Harmon et al., 2008; Paradis et al., 2004). The ancestral states were reconstructed by Ace function, using maximum likelihood optimization. The output from R was mapped onto the Bayesian phylogenetic tree with TreeExtender v1.03 (Verbruggen, 2009), using a simple list parser (option – p list). The ancestral states of discrete data (order of lobe division and biogeography) were reconstructed in the program BayesTraits (Pagel and Meade, 2006). The ancestral state probabilities were calculated using BayesMultiState in a maximum likelihood framework (using the 'addNode' command). We adjusted the 'Mltries' parameter to 100 to increase the number of optimalisation attempts. The BayesTraits output was mapped onto the Bayesian tree with TreeExtender v1.03, using a BayesTraits parser (option – p bt). Finally, evolution of both continuous and discrete characters was traced on a phylogenetic tree as colours along a gradient with TreeGradients v1.03 (Verbruggen, 2009). Evolution of geographic origin was traced along the Bayesian phylogenetic tree using maximum parsimony reconstruction in the Mesquite software package, v2.72 (Maddison and Maddison, 2006).

3. Results

3.1. Exploration of the phylogenetic data

The concatenated matrix contained 41 taxa and 3 genes: SSU rDNA, *psa*A, and *cox*III. The matrix was 3285 bp long and was

Table 1
Specifications, evolutionary models and model parameters obtained for different datasets.

	Complete dataset	SSU rDNA	*psa*A	*cox*III
Number of sites	3285	1782	920	583
Number of variable sites	367 (11.2%)	148 (8.3%)	173 (18.8%)	46 (7.9%)
Number of parsimony-informative sites	222 (6.8%)	97 (5.4%)	96 (10.4%)	29 (5.0%)
Likelihood mapping results (fully resolved/fully unresolved Quartets in %)	96.5/0.9	93.0/2.0	94.7/2.0	21.4/78.2

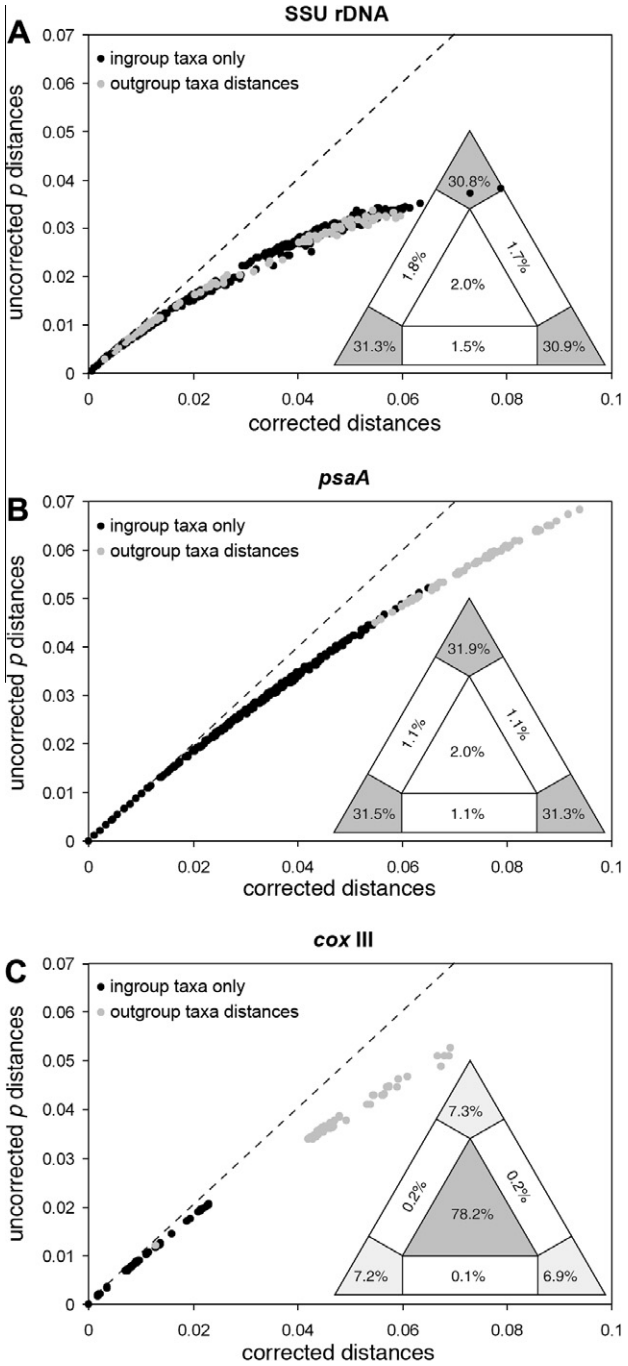

Fig. 2. Analysis of substitutional saturation. The graphs visualize the saturation of the SSU rRNA (A), *psa*A (B) and *cox*III (C) datasets by plotting ML-corrected distances against uncorrected p-distances. The pairwise genetic distances are shown for both ingroup taxa only (black dots) and ingroup + outgroup (*Staurastrum*) sequences (grey dots). The triangles in the lower right of the graphs illustrate likelihood mapping results. The values in the panels indicate proportion of fully resolved (corners), partially resolved (along the sides), and fully unresolved quartets (in the centre).

95% filled for the SSU rDNA data, 98% filled for the *psa*A data, and 100% filled for the *cox*III data. The loci differed considerably in the amount of phylogenetic signal (Table 1). The *psa*A dataset contained more than twice the amount of both variable and parsimony informative sites than the other genes. Testing the data partitions for substitution saturation (distribution of the uncorrected vs. corrected distances; Fig. 2) revealed a nearly linear correlation indicating low saturation in both *psa*A and *cox*III data. However, the saturation plot of SSU rDNA (Fig. 2A) was found to level off with increasing genetic distance, indicating significant saturation of this locus. Obvious differences among three analysed loci were found when comparing pairwise genetic distances of ingroup taxa only with those distances counted for ingroup + outgroup (*Staurastrum*) sequences. No differences were observed in SSU rDNA dataset, but in both *psa*A and *cox*III genes pairwise sequence divergences of the ingroup taxa was found to be considerably lower than of the ingroup + outgroup sequences (Fig. 2). In other words, whereas SSU rDNA failed to differentiate *Micrasterias* from closely related genus *Staurastrum*, the distinction of *Micrasterias* was clearly demonstrated in both the *psa*A and, in particular, the *cox*III gene. Results of likelihood mapping are presented in Table 1 and Fig. 2. A strong phylogenetic signal was detected in the SSU rDNA and *psa*A loci (93.0% and 94.7% of fully resolved quartets, respectively). On the other hand, only 21.4% of fully resolved quartets were identified for the *cox*III locus, indicating very weak phylogenetic signal. The combined alignment of all 3 loci had the highest percentage of fully resolved quartets (96.5%) and only 0.9% of quartets fully unresolved.

3.2. Phylogenetic analyses

Visual inspection of single-locus trees revealed that almost all moderately to well-supported clades (those receiving posterior probability values $\geqslant 0.95$) were monophyletic in all SSU rDNA, *psa*A, and *cox*III Bayesian trees (i.e. all members of the each well-resolved clade in the phylogeny of particular locus were not inferred in separate, well-resolved lineages in the phylogenetic analyses of two other loci). The only two exceptions were the rival phylogenetic positions of the clade encompassing *Micrasterias anomala* and *Micrasterias apiculata* (clade B in Fig. 3) and the clade comprising *Micrasterias furcata*, *Micrasterias pinnatifida*, and *Staurodesmus dickiei* (clade A4 in Fig. 3). The clade B was inferred to be sister to the clade A in SSU rDNA, the clade H in *psa*A, and the clade C in *cox*III analyses. Similarly, the clade A4 was nested within the clade A in both SSU rDNA and *psa*A analyses, but was inferred to be sister to the clade E in *cox*III analysis. Nevertheless, the general congruence of the single-locus phylogenies justified a combined data approach.

The concatenated SSU rDNA, *psa*A, and *cox*III tree constructed by Bayesian inference on partitioned datasets led to the recognition of eight well-resolved lineages designated as clades A–H (Fig. 3), receiving a high statistical support in all three single-locus phylogenies, as well. The clade A comprised the highest number of investigated *Micrasterias* species, showing two distinct morphologies. About half of the species could be defined by having medium-sized, shallowly divided cells with broad polar lobes; these were

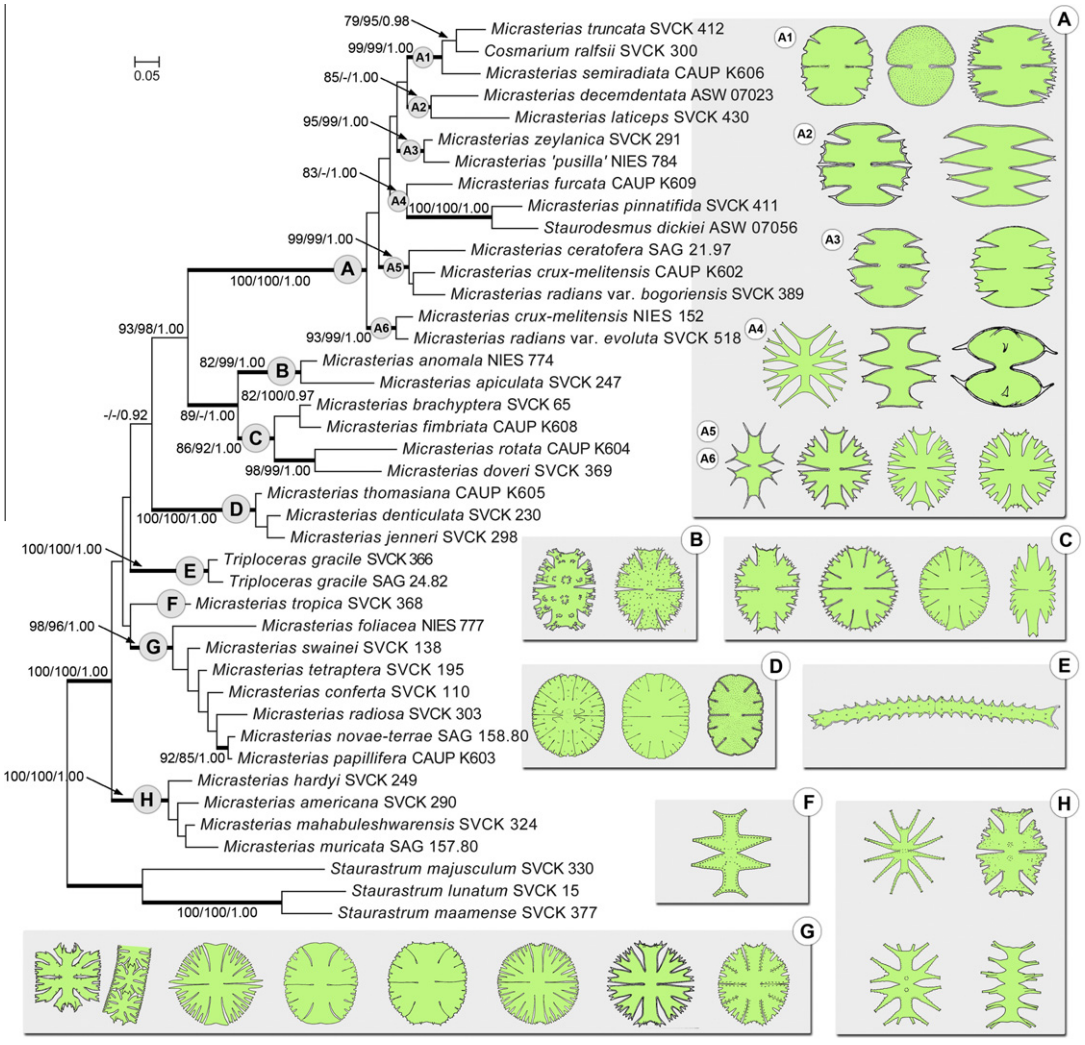

Fig. 3. Bayesian analysis based on the combined and partitioned SSU rDNA, *psa*A, and *cox*III dataset using a GTR + Γ model for SSU rDNA region and 3rd codon position of *psa*A gene, F81 + Γ model for 1st and 2nd codon position of *psa*A and *cox*III genes, and HKY model for 3rd codon position of *cox*III gene. The doublet model is applied for the stem regions in the SSU rDNA region. Values at the nodes indicate statistical support estimated by three methods – maximum likelihood bootstrap (left), maximum parsimony bootstrap (in the middle) and MrBayes posterior node probability (right). Thick branches represent nodes receiving the highest PP support (1.00). Species affiliation to eight clades (A–H; including six sub-clades A1–A6) is indicated. Morphology of investigated strains is given in the boxes next to the tree, according to their affiliation to the particular clades. The order of the species in the tree (from above to down) corresponds to the order of the cells illustrated in the boxes (from left to right). Scale bar – estimated number of substitutions per site.

members of sub-clades A1–A3. By contrast, the other species had typically large, deeply divided cells, with narrow polar lobes (the members of the sub-clades A5 and A6). Apart from the members traditionally assigned to the genus *Micrasterias*, two species classified to different desmid genera were inferred within the clade A. The strain of *Cosmarium ralfsii* (SVCK 300) was related to *Micrasterias truncata* and *Micrasterias semiradiata* (sub-clade A1). This species primarily differs from *Micrasterias* by the complete absence of incisions dividing semicells into separate lobes. The second species *S. dickiei* was inferred within the sub-clade A4, forming a highly resolved clade with *M. pinnatifida*. *S. dickiei* differs from all the *Micrasterias* species in several prominent morphological features. It has elliptic, triradiate cells without incisions and bears three distinct spines.

The clade B consisted of only two species, *M. anomala* and *M. apiculata*, characterized by a group of 3–7 stouter spines in the middle of the cell, above the isthmus. The clade C comprised the species having unequally branched lateral lobes, with the upper lobe more divided than the lower one. Moreover, this clade contained the largest known species of the genus (*M. rotata* and *Micrasterias doveri*). The clade D could be well defined by comprising species having oval to oblong cells with closed incisions (*M. thomasiana*, *Micrasterias denticulata* and *Micrasterias jenneri*). The clade E was formed by two strains of *Triploceras gracile* (SVCK 377 and SAG 24.82). The genus *Triploceras* comprises elongate, cylindrical cells bearing several whorls of mamillate protuberances, each bearing one or more short spines. It is morphologically very distinct, clearly differentiated from all the *Micrasterias* species by the absence of lateral lobes. The clade F consisted of single *Micrasterias* species, *M. tropica*. This species has been characterized by unbranched lateral lobes and a polar lobe with two long processes. Even if we found only a single member of clade F, it probably consists of more taxa not included in this analysis. These morphologically similar but distinct biological entities were formally described as different varieties of *M. tropica* (Krieger, 1939).

The remaining *Micrasterias* species were inferred as members of clades G and H. The former clade comprised seven species that could be characterized by having deeply incised cells, typically divided to the high-order levels. The majority of strains belonging to this clade had unevenly divided lateral lobes, with the upper lateral

lobules usually being broader and divided to a higher level than the lower ones. *Micrasterias foliacea*, a single known filamentous species, was inferred to have a basal position in this clade. The clade H consisted of four species with deeply divided cells, open incisions, and very broad polar lobes. The prominent joint morphological feature of this group was the presence of two short accessory processes arising at the end of the polar lobes (Fig. 3).

3.3. Evolution of morphological characters

To better understand the evolutionary history and morphological diversification of the genus, we mapped the selected morphological characters (such as branching pattern, cell complexity, and cell length) along the phylogenetic tree. First, we analysed the evolution of the branching pattern (Fig. 4A). The maximum likelihood reconstruction showed a strong phylogenetic pattern of this feature, indicating its high evolutionary significance. Species of the clades A and H showed a clear tendency to produce less divided cells. With the single exception of *Micrasterias radians* var. *bogoriensis*, all species included in these clades had at most 2nd order divided lateral lobes, which terminated in four lobules. Four out of the total six species with cells bearing undivided lateral lobes, or missing such lobes completely, were inferred solely within the clade A. Conversely, species with highly lobed cells were included in clades B–D, and G. Lateral lobes of species belonging to these clades had at least 3rd order divided lateral lobes. Species belonging to the clade D had the highest number of terminal lobules (16 in *M. thomasiana* and 15 in *M. denticulata*). A completely different pattern was observed in the evolution of cell complexity. The maximum likelihood reconstruction illustrated low correlation of this morphological indicator with the phylogenetic pattern (Fig. 4B). Species having morphologically simple and complex cells were intermixed in almost all lineages. For example, the clade A contained both species with highly complex cells (such as *M. furcata* and *M. radians* var. *bogoriensis*) and morphologically simple species (*Micrasterias laticeps*, *S. dickiei*). Similarly, the clade D comprised three species with profoundly different cell complexity values (*M. thomasiana*, 2.45; *M. denticulata*, 1.93; and *M. jenneri*, 1.34). The analysis of cell length evolution illustrated that the clades A and G comprised smaller species, with the average cell length not exceeding 153 (clade A) and 175 μm (clade G), respectively. By contrast, species with large cells (more than 200 μm in length) were inferred in clades B, C, and E (Fig. 4C).

3.4. Biogeography

Although the majority of investigated *Micrasterias* species (58%) have cosmopolitan distribution (Krieger, 1939), mapping individual phycogeographic regions on the concatenated phylogeny (MP method; Fig. 4D) revealed distinct biogeographic patterns. North America was represented by the highest number of species (79% of analysed *Micrasterias* species). All the North American endemics—*Micrasterias swainei*, *Micrasterias novae-terrae*, and *Micrasterias muricata*—occupied the basal clades G and H, indicating the potential origin of the genus on this continent. The second richest region was Indo-Malaysia/Northern Australia, with the occurrence of 71% of analysed *Micrasterias* species. In contrast to North American endemics, both Indo-Malaysian endemics (*M. radians* var. *bogoriensis* and *Micrasterias ceratofera*) were clustered into the clade A. Further, 14 of the 15 species included in the clade A were documented to occur in the Indo-Malaysian/Northern Australian region, suggesting possible origin of the lineage in this geographic area. The maximum likelihood reconstruction of ancestral distributions, analysing preferences to temperate, tropical, and polar biogeographic regions, matched well with the MP mapping described above (Fig. 4D). The analysis suggested an origin of the genus in temperate region, and that the most speciation events of the lineage A happened in the tropics. Biogeographic mapping further suggested additional speciation events in temperate regions (e.g., lineages A1 and A2) and no speciation events in polar areas.

4. Discussion

4.1. Genetic diversification of the genus Micrasterias

In this paper, we present a scenario for the evolution of the desmid genus *Micrasterias*, based on the robust phylogeny of 41 taxa. Omitting a number of infraspecific, morphologically little differentiated taxa, we can conclude that our study included more than half of all described traditional species of this genus. An addition of more species could obviously improve the phylogenetic reconstruction, but more strains have not been available in the public culture collections. Nevertheless, some apparent trends regarding the rate of morphological evolution and evolutionary differentiation of the genus were recovered. In particular, our results indicated a single origin, that is, monophyly, of the genus *Micrasterias* that was, however, at least three times followed by substantial morphological transformations leading to the evolution of morphologically very different species. In two of these cases (*C. ralfsii* and *S. dickiei*) the closest relatives of these morphologically simplified forms were detected (Fig. 2) so that the phenotypic transformations leading to the origin of these taxa may be traced (see Section 4.2).

This study was primarily focused on the diversification of the genus so that we did not analyse the exact phylogenetic position of *Micrasterias* within Desmidiales. However, considering all the three morphologically anomalous species (i.e. *C. ralfsii*, *S. dickiei*, and *T. gracile*) as members of the genus *Micrasterias*, all *Micrasterias* taxa tend to form a single monophyletic clade. Even though there was no significance, the monophyly of the genus was indicated on the recent phylogenetic studies dealing with SSU rDNA (Neustupa et al., 2010), *rbc*L (Gontcharov and Melkonian, 2011), and various concatenated multigenic datasets (Gontcharov and Melkonian, 2008; Hall et al., 2008). The only exception was the phylogenetic position of SVCK 103 strain of *Hyalotheca mucosa* that was nested within the genus *Micrasterias* in SSU rDNA phylogram of Neustupa et al. (2010). To verify the affinity of this strain to *Micrasterias*, we acquired it from the culture collection and obtained the SSU rDNA, *psa*A, and *cox*III sequences. Along with the verification of the SSU rDNA sequence published in GenBank database (Accession No. AJ428121), we determined that the *psa*A and *cox*III sequences were so divergent from sequences of all the *Micrasterias* taxa, as well as from all related *Staurastrum* sequences, that the SVCK 103 strain may safely be considered unrelated to *Micrasterias*. Moreover, morphological investigation of SVCK 103 strain revealed its incorrect determination as *H. mucosa*, which should be changed to *Spondylosium* sp.

According to our phylogenetic analysis, the genus *Micrasterias* comprises of at least eight lineages. Statistical support for the backbone of the phylogenetic tree was relatively low, which precluded identification of a basal, ancestral lineage. Nevertheless, clustering of individual *Micrasterias* species into eight lineages was well supported, which allowed us to confront our findings with traditional ideas on the diversification of the genus. Several attempts were made in the past to divide the genus into infrageneric taxa on the basis of their morphological properties. The taxonomic conceptions varied, ranging from a small number of subgenera containing many species (Cooke, 1886; Hirano, 1959; Prescott et al., 1977; Turner, 1892) to a large number of infrageneric groups comprising few or even a single species (Krieger, 1939). According to the phylogeny presented in this study, we can conclude that the

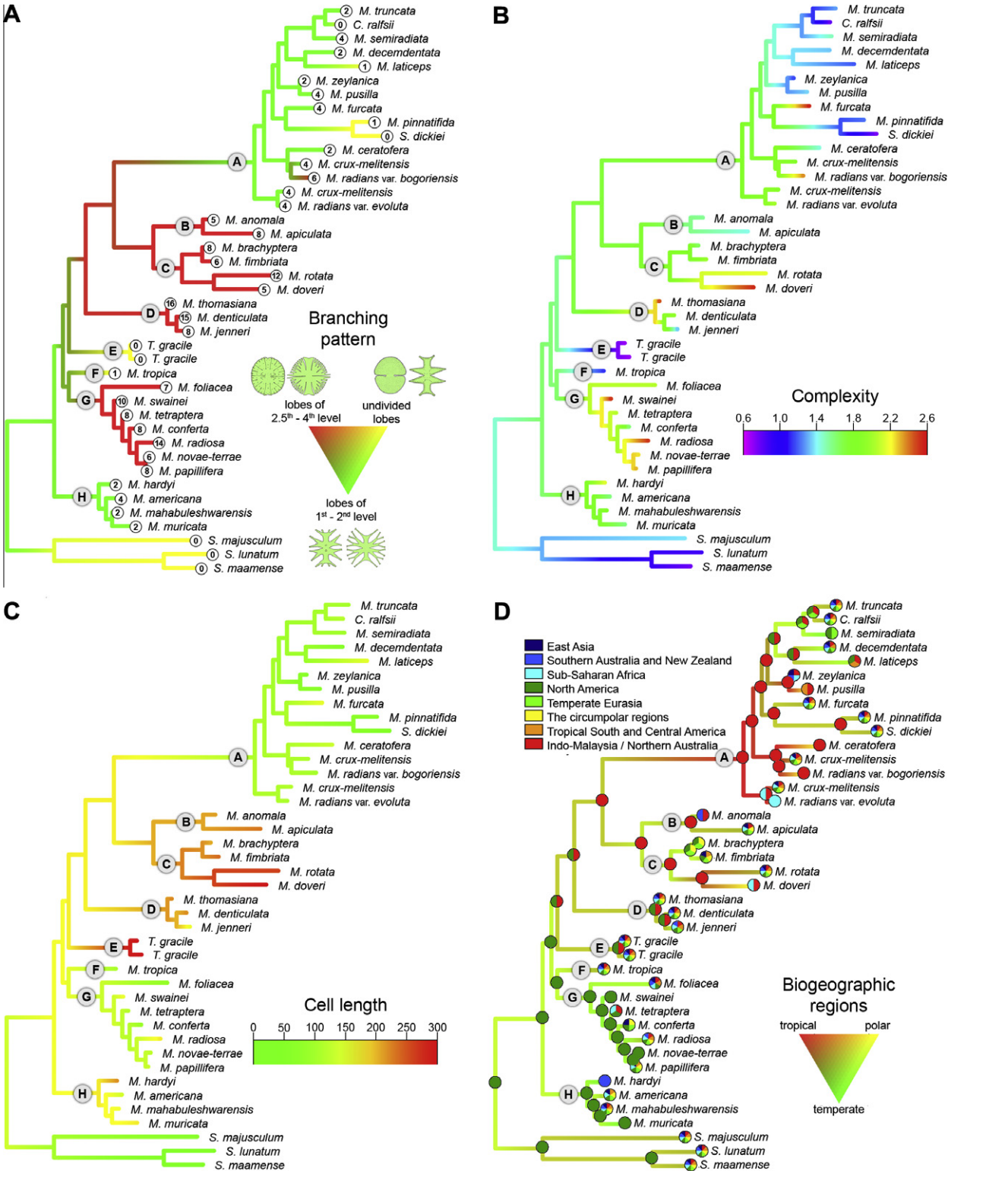

Fig. 4. Evolution of selected morphological characters and geographical distribution mapped onto the phylogenetic tree (maximum likelihood method). (A) Estimated evolution of branching pattern. Probabilities for ancestral branching pattern are given in colour. Numbers at the end of branches reflects the total number of lobules in one semicell. (B) Estimated evolution of the complexity of cell shape. (C) Estimated evolution of average cell length. (D) Geographical distribution. Estimated probabilities for ancestral distribution in three biogeographic regions (temperate regions, polar regions and tropics) are given in colour. Pie charts indicate the ancestral maximum parsimony estimations for the distribution in eight geographical zones.

classification proposed by Krieger (1939) turned out to be best supported by the molecular data. Interestingly, some of the subgeneric lineages were already recognized in the past, based on their morphological distinctness. For example, the lineage H, characterized by species with short accessory processes on their polar lobes, was distinguished as either the subgenus *Schizocystis* (Prescott et al., 1977; West and West, 1905) or, informally, as the "*Micrasterias americana*-Gruppe" (Krieger, 1939). Similarly, species

having cells with broad polar lobes (lineages A1–A3) were traditionally classified into the subgenus *Holocystis* (Prescott et al., 1977; Ralfs, 1848; West and West, 1905) and the *M. truncata*-Gruppe (Krieger, 1939). By contrast, *M. jenneri* was never classified into a joint group with *M. thomasiana* and *M. denticulata*, despite the morphological similarities that seems obvious (Prescott et al., 1977; Tyler, 1970).

4.2. Implications for the morphological evolution in protists

Micrasterias is an exceptionally suitable model organism for investigating the patterns of morphological evolution in protists. First, the members of this genus have large and spectacularly shaped cells. Therefore, unlike most protist genera, there is a well-defined species concept enabling correct determination and delimitation of species. Second, due to its long-term investigations, the suggested morphological evolution hypotheses could be confronted with the results of population studies and morphogenetic experiments (e.g., Kallio, 1949, 1951; Sormus and Bicudo, 1974). Mapping the morphological diversification of the genus on phylogenetic pattern revealed clear differences in the phylogenetic signal of selected phenotypic features (i.e. differences in the tendency for genetically related species to resemble each other). Whereas several morphological features clearly correlated with the phylogeny (e.g., the branching pattern and average cell length; Fig. 4A and C), the others seem to have evolved more or less independently of phylogeny. A good example is the cell complexity that was found uncorrelated with phylogenetic data. Interestingly, the recently published ecophysiological study focusing on the morphological variation in two selected desmid species (Černá and Neustupa, 2010) demonstrated that the cell complexity may reflect adaptive morphological responses to external factors such as the pH level of the environment.

The most intriguing pattern detected in our combined phylogenetic and morphological analyses has been the existence of several periods of accelerated morphological evolution during the diversification of the genus. In these periods, substantial morphological transformations led to the speciation of three morphologically distinct species, traditionally classified into different desmid genera. Whereas the speciation of two of these species (*C. ralfsii* and *S. dickiei*) occurred relatively recently, the third one (*T. gracile*) originated early in the evolution of the *Micrasterias* lineage. Evolution of *C. ralfsii* within the genus *Micrasterias* may be explained by comparison of this species with closely related *M. truncata* and *M. semiradiata*. These taxa show relatively similar cell shapes with shallow incisions, broad polar lobes, and relatively similar cell lengths (Figs. 3 and 4C). The likeliest evolutionary scenario is therefore the successive reduction of lobe incisions, leading to the speciation into the smooth, unincised form typical for *C. ralfsii* (Fig. 5A). Cells of *C. ralfsii* are actually much larger than cells of other *Cosmarium* species; in addition, they possess morphologically very similar plastids to those of traditional *Micrasterias* species (Ralfs, 1848; Šťastný, 2009).

Morphological evolutionary transformation of *Micrasterias*-like morphotypes into *S. dickiei* is much less straightforward. In contrast to *Micrasterias* species, *S. dickiei* has unincised, triradiate cells bearing several distinct incisions. Therefore, during the speciation of this species the cells had to reduce their lobe incisions, as well as to change the biradiate cell outline to a triradiate form. Although the rapid morphological transformation into the triradiate form may seem unlikely, triradiate forms of several *Micrasterias* species have been reported in nature (e.g., Heimans, 1942; Skuja, 1964; West, 1889; West and West, 1905). In addition, laboratory experiments illustrated artificial production of triradiate forms either by forced diploidisation (Kallio, 1949, 1951) or by continuous exposure to high intensity illumination (Kallio, 1953). Moreover, formation of triradiate forms was shown to be accompanied by shape simplification, typical for the morphology of *S. dickiei*. For example, Teiling (1956) found the strongly reduced triradiate cell of *Micrasterias mahabuleshwarensis* in a sample of an alpine lake. Therefore, the most probable evolutionary explanation for the origin of *S. dickiei* would be the natural diploidisation of the *Micrasterias*-like ancestor, leading to the production of triradiate cells with reduced lobulation patterns (Fig. 5B). Interestingly, Sormus and Bicudo (1974) described spontaneous formation of simplified, triradiate semicells in a population of *M. pinnatifida* that was inferred as a close relative of *S. dickiei* on the basis of the molecular data. This observation may indicate the evolutionary potential of *M. pinnatifida*-like ancestor to speciate into the triradiate species such as *S. dickiei*.

The other period of an accelerated morphological evolution occurred during the speciation of *T. gracile*, a species typified by its long cylindrical cells (Krieger, 1937). Considering its phylogenetic position within the *Micrasterias* lineage, one could assume that *Triploceras* cells may represent residual polar lobes of ancestral *Micrasterias* species. This idea may be supported by morphogenetic experiments of Kallio and Heikkilä (1969), who artificially produced aradiate forms of *M. torreyi* by irradiation with ultraviolet light. These forms resembled *Triploceras* species, with cells consisting solely of polar lobes. Moreover, aradiate cells were also obtained from natural samples (Waris and Kallio, 1964), suggesting that environmental disturbances causing formation of these forms may also occur in natural habitats. The evolutionary scenario leading to evolution of *Triploceras* forms from a *Micrasterias*-like ancestor thus implies formation of aradiate cells, followed by the prolongation of polar lobes and creation of spiny mamillate protuberances on their surface (Fig. 5C). Interestingly, both the production of larger polar lobes and the formation of spine-like processes were observed in aradiate cells of *M. americana* (Kallio, 1960; Waris and Kallio, 1964).

These evolutionary scenarios indicate that morphology of desmid species could abruptly change during a relatively short period of its evolution. Such evolutionary patterns would be inconsistent with the theory of a long-term morphological stasis of protist species raised by Fenchel and Finlay (2006) and Martín-González et al. (2008). Various morphogenetic experiments discussed above suggest that rapid morphological changes of desmid populations could be induced by various stress conditions, such as ultraviolet light and cold shocks (Kallio, 1949), as well as by natural polyploidisation. Although the importance of polyploidy in plant speciation has been generally accepted (Rieseberg and Willis, 2007), almost nothing is known of its relevance in the speciation of protists. There are only a few papers dealing with ploidy level estimations of protists. Luckily, several such studies investigated the chromosome numbers of *Micrasterias* species (Kasprik, 1973; King, 1960; Waris, 1950). Surprisingly, large differences were noticed not only among particular *Micrasterias* species (chromosome numbers ranging from 24 to 230), but occasionally also among different isolates of a single species (e.g., *M. americana*). These differences may provide an indirect evidence of possible polyploid origin of *Micrasterias* species (Kallio, 1954).

4.3. Biogeography

From a biogeographic point of view, desmids represent possibly the best-studied microalgal group (Coesel and Krienitz, 2008). In the early 20th Century, West (1909) stated that no group of freshwater algae exhibit such pronounced biogeographic patterns as desmids. Later on, Krieger (1939) distinguished seven desmid floral regions, characterized by similarities in distribution patterns of particular desmid taxa. These regions were clearly differentiated by the proportion of endemic species. Although Eastern Asia,

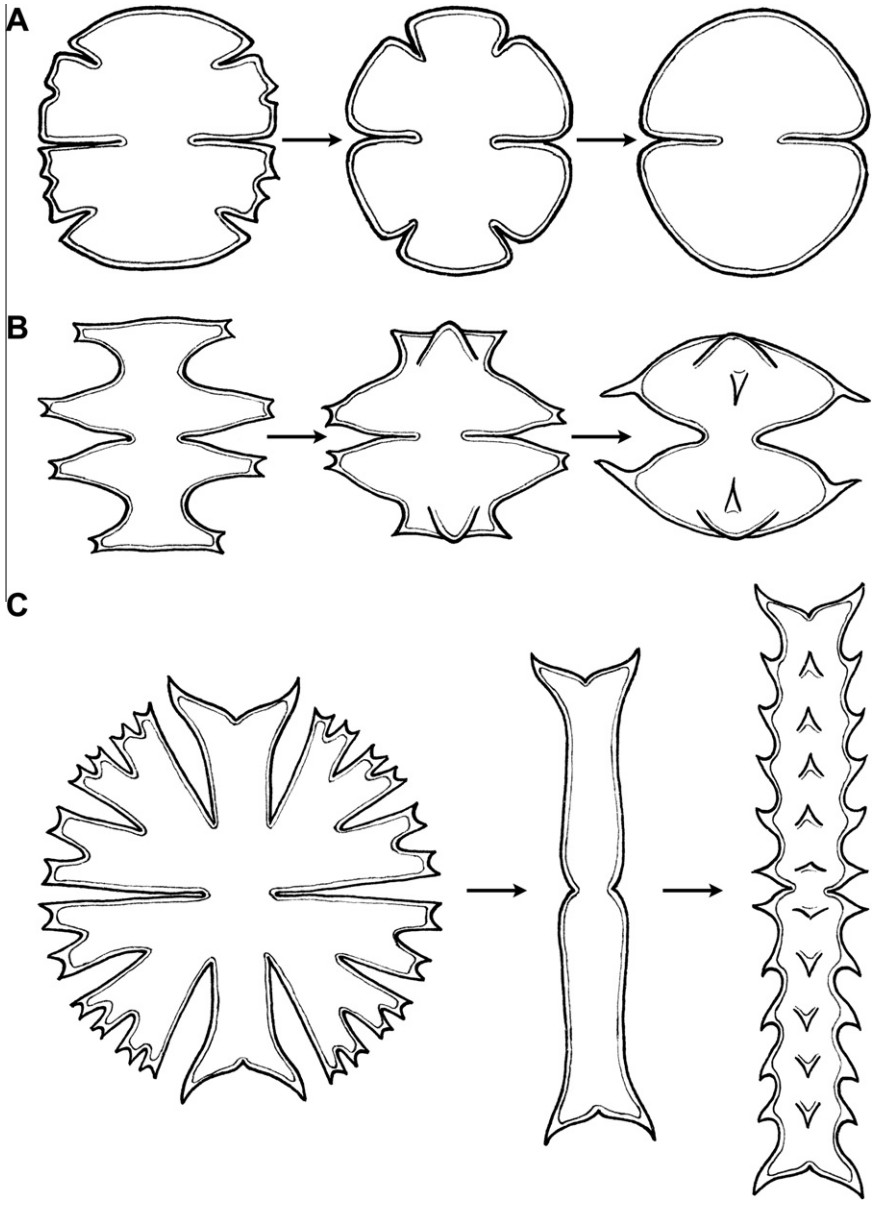

Fig. 5. A hypothetical evolutionary scenario of morphological transformations leading to the speciation into the three morphologically distinct species. (A) Speciation of *M. truncata* ancestor into the *Cosmarium ralfsii*. (B) Speciation of *M. pinnatifida* ancestor into the *Staurodesmus dickiei*. (C) Speciation of *Micrasterias* ancestor into the *Triploceras gracile*. See text for details (Section 4.2).

Northern and tropical Southern America, and Indo-Malaysia were characterized by a high number of presumably endemics, temperate Eurasia and circumpolar regions housed only few endemic species (Coesel, 1996). These differences were mainly ascribed to the Pleistocene glaciations that contributed to the extinction of many taxa in cold and temperate regions. A strong latitudinal gradient of species diversity was proposed both in terms of regional species richness as well as in number of endemics. The diversity optima in the tropics were considered to signify the evolutionary origins of desmids in these regions (Coesel, 1996). Interestingly, contrary to this hypothesis of tropical origin of desmids, our combined molecular phylogenetic and species distribution data suggested that the genus *Micrasterias* may have evolved in North America (Fig. 4D). This hypothesis is corroborated by the presence of rich desmid flora in North America and retention of species endemic to this region at the base of the phylogenetic tree. Ancient members of the genus might then subsequently migrate to other geographical regions including the tropics, where they speciated into the numerous phylogenetically related species.

4.4. Taxonomical consequences

Three morphologically distinct species (*C. ralfsii*, *S. dickiei*, and *T. gracile*) were shown to be nested within the genus *Micrasterias*. The substantial morphological differences of these taxa from other *Micrasterias* species have led desmidiologists to classify them as members of morphologically simpler genera. The presented phylogenetic data indicate that *C. ralfsii* and *S. dickiei* evolved relatively recently from other *Micrasterias* taxa. Since the type species (lectotypes) of both *Cosmarium* and *Staurodesmus* (i.e. *Cosmarium undulatum* and *Staurodesmus triangularis*, respectively) were inferred as members of unrelated clades (Gontcharov and Melkonian, 2011), we formally transfer *C. ralfsii* and *S. dickiei* into the genus *Micrasterias*, along with the emendation of the genus description. On the other hand, *T. gracile* originated early in the evolution of *Micraste-*

rias. Although the *psa*A and *cox*III sequence data clearly showed a close relationship of *T. gracile* to the genus *Micrasterias*, we still cannot be sure that it is truly nested within this genus. Although the morphogenetic experiments of Kallio and Heikkilä (1972) indicated the probable origin of *Triploceras* from *Micrasterias* ancestors by blocking of morphogenetic modules driving development of lateral cell lobes, poor statistical support for the backbone of the phylogenetic tree does not preclude the basal position of *Triploceras* in the phylogram, and inferential evolution of *Micrasterias* species from the *Triploceras*-like ancestor. Therefore, to avoid new, potentially superfluous names being introduced, we do not formally transfer *T. gracile* into the genus *Micrasterias*.

Micrasterias C. Agardh ex Ralfs emend. Skaloud, Nemjova, Vesela, Cerna et Neustupa.

Emended Diagnosis: Cells are small to large, usually solitary (*M. foliacea* is filamentous), with a very deep median constriction (isthmus). Other shallow or deep incisions usually divide each semicell into apical lobe and two lateral lobes, which could be further subdivided. Semicells of *M. ralfsii* and *M. dickiei* are undivided. Cells are usually flattened and disc-shaped (*M. dickiei* has elliptic, triradiate cells). Some species have small or large protuberances, processes, or spines. There is usually one chloroplast per semicell, containing few to numerous pyrenoids. The nucleus is localized in the isthmus.

Micrasterias ralfsii (Brébisson ex Ralfs) Skaloud, Nemjova, Vesela, Cerna et Neustupa comb. nov.

Basionym: *Cosmarium ralfsii* Brébisson ex Ralfs, 1848; Brit. Desmid, p. 93, pl. XV, Fig. 3.

Synonym: *Pleurotaeniopsis ralfsii* (Ralfs) De Toni, 1889; Syll. Alg. 1, p. 911.

Micrasterias dickiei (Ralfs) Skaloud, Nemjova, Vesela, Cerna et Neustupa comb. nov.

Basionym: *Staurastrum dickiei* Ralfs, 1848; Brit. Desmid, p. 123, pl. XXI, Fig. 3a and b.

Synonyms: *Staurodesmus dickiei* (Ralfs) Lillieroth, 1950; Acta Limnol. 3, p. 264.

Acknowledgments

We are greatly indebted to Monika Engels for kind provision of a number of strains from the SVCK culture collection. Moreover, Maike Lorenz (SAG culture collection), Fumie Kasai (NIES culture collection), Barbara Melkonian (CCAC culture collection) and Jerry Brand (UTEX culture collection) are thanked for providing additional strains used it this study. We are grateful to the anonymous reviewers for the constructive comments. The study has been supported by the Grant No. 206/09/0906 of the Czech Science Foundation and the grant No. MSM0021620828.

Appendix A. Supplementary material

Supplementary data associated with this article can be found, in the online version, at doi:10.1016/j.ympev.2011.08.018.

References

Agardh, C.A., 1827. Aufzählung einiger in den östreichischen Ländern gefundenen neuen Gattungen und Arten von Algen, nebst ihrer Diagnostik und beigefügten Bemerkungen. Flora 10, 625–646.

An, S.S., Friedl, T., Hegewald, E., 1999. Phylogenetic relationships of *Scenedesmus* and *Scenedesmus*-like coccoid green algae as inferred from ITS-2 rDNA sequence comparisons. Plant Biol. 1, 418–428.

Coesel, P.F.M., 1996. Biogeography of desmids. Hydrobiologia 336, 41–53.

Coesel, P.F.M., Krienitz, L., 2008. Diversity and geographic distribution of desmids and other coccoid green algae. Biodivers. Conserv. 17, 381–392.

Cooke, M.C., 1886. British Desmids. A Supplement to British Fresh-Water Algae. Williams and Norgate, London.

Černá, K., Neustupa, J., 2010. The pH-related morphological variations of two acidophilic species of Desmidiales (Viridiplantae) isolated from a lowland peat bog, Czech Republic. Aquat. Ecol. 44, 409–419.

Darienko, T., Gustavs, L., Mudimu, O., Menendez, C.R., Schumann, R., Karsten, U., Friedl, T., Pröschold, T., 2010. *Chloroidium*, a common terrestrial coccoid green alga previously assigned to *Chlorella* (Trebouxiophyceae, Chlorophyta). Eur. J. Phycol. 45, 79–95.

Denboh, T., Hendrayanti, D., Ichimura, T., 2001. Monophyly of the genus *Closterium* and the order Desmidiales (Charophyceae, Chlorophyta) inferred from nuclear small subunit rDNA data. J. Phycol. 37, 1063–1072.

Edgar, R.C., 2004. MUSCLE: multiple sequence alignment with high accuracy and high throughput. Nucl. Acids Res. 32, 1792–1797.

Fenchel, T., Finlay, B.J., 2006. The diversity of microbes: resurgence of the phenotype. Phil. Trans. Roy. Soc. B 361, 1965–1973.

Gontcharov, A.A., 2008. Phylogeny and classification of Zygnematophyceae (Streptophyta): current state of affairs. Fottea 8, 87–104.

Gontcharov, A.A., Melkonian, M., 2008. In search of monophyletic taxa in the family Desmidiaceae (Zygnematophyceae, Viridiplantae): the genus *Cosmarium* Corda ex Ralfs. Am. J. Bot. 95, 1079–1095.

Gontcharov, A.A., Melkonian, M., 2011. A study of conflict between molecular phylogeny and taxonomy in the Desmidiaceae (Streptophyta, Viridiplantae): Analyses of 291 *rbc*L sequences. Protist 162, 253–267.

Gontcharov, A.A., Marin, B., Melkonian, M., 2003. Molecular phylogeny of conjugating green algae (Zygnemophyceae, Streptophyta) inferred from SSU rDNA sequence comparisons. J. Mol. Evol. 56, 89–104.

Hall, J.D., Karol, K.G., McCourt, R.M., Delwiche, C.F., 2008. Phylogeny of the conjugating green algae based on chloroplast and mitochondrial nucleotide sequence data. J. Phycol. 44, 467–477.

Harmon, L.J., Weir, J.T., Brock, C.D., Glor, R.E., Challenger, W., 2008. GEIGER: investigating evolutionary radiations. Bioinformatics 24, 129–131.

Heimans, J., 1942. Triquetrous forms in the genus *Micrasterias*. Blumea 2 (Suppl.), 52–63.

Hepperle, D., 2004. SeqAssem©. A Sequence Analysis Tool, Contig Assembler and Trace Data Visualization Tool for Molecular Sequences. <http://www.sequentix.de>.

Hirano, M., 1959. Flora Desmidiarum Japonicarum. Contr. Biol. Lab. Kyoto 7, 226–301.

Huss, V.A.R., Frank, C., Hartmann, E.C., Hirmer, M., Kloboucek, A., Seidel, B.M., Wenzeler, P., Kessler, E., 1999. Biochemical taxonomy and molecular phylogeny of the genus *Chlorella* sensu lato (Chlorophyta). J. Phycol. 35, 587–598.

Jobb, G., 2008. TREEFINDER version of October 2008. Munich, Germany, Distributed by the author at <www.treefinder.de>.

Kallio, P., 1949. Artificially produced binuclear, diploid and a nuclear desmids. Arch. Soc. Zool.-Bot. Fenn. Vanamo 2, 42–44.

Kallio, P., 1951. The significance of nuclear quantity in the genus *Micrasterias*. Arch. Soc. Zool.-Bot. Fenn. Vanamo 24, 1–122.

Kallio, P., 1953. The effects of continued illumination on desmids. Arch. Soc. Zool.-Bot. Fenn. Vanamo 8, 58–74.

Kallio, P., 1954. Morphogenetic studies in *Micrasterias rotata* (Grey.) Ralfs var. *evoluta* Turner (Desmidiaceae). Arch. Soc. Zool.-Bot. Fenn 8, 118–122.

Kallio, P., 1960. Morphogenetics of *Micrasterias americana* in clone culture. Nature, London 187, 164–166.

Kallio, P., Heikkilä, H., 1969. UV-induced facies changes in *Micrasterias torreyi*. Öster. Bot. Zeit. 116, 226–243.

Kallio, P., Heikkilä, H., 1972. On the effect of elimination of nuclear control in *Micrasterias*. In: Bonotto, S., Goutier, R., Kirchmann, K., Maisin, J.R. (Eds.), Plant Cells. Academic Press, Inc., New York, pp. 167–192.

Kasprik, W., 1973. Beitrge zur Karyologie der Desmidiaceen – Guttung *Micrasterias* Ag. Beih. Nova Hedwigia 42, 115–137.

King, G.C., 1960. The cytology of the desmids: the chromosomes. New Phytol. 59, 65–72.

Krieger, W., 1937. Die Desmidiaceen Europas mit Berücksichtigung der aussereuropäischen Arten. Band 13. Abteilung 1, Teil 1, Lieferung 1 of Dr. Rabenhorst's Kryptogamen-Flora von Deutschland, Österreich und der Schweiz. Akademische Verlagsgeselschaft M.B.H., Leipzig.

Krieger, W., 1939. Die Desmidiaceen Europas mit Berücksichtigung der aussereuropäischen Arten. Band 13. Abteilung 1, Teil 2, Lieferung 1 of Dr. Rabenhorst's Kryptogamen-Flora von Deutschland. Österreich und der Schweiz. . Akademische Verlagsgeselschaft M.B.H., Leipzig.

Krienitz, L., Hegewald, E.H., Hepperle, D., Huss, V.A.R., Rohr, T., Wolf, M., 2004. Phylogenetic relationship of *Chlorella* and *Parachlorella* gen. Nov. (Chlorophyta, Trebouxiophyceae). Phycologia 43, 529–542.

Kumar, S., Dudley, J., Nei, M., Tamura, K., 2008. MEGA: a biologist-centric software for evolutionary analysis of DNA and protein sequences. Brief. Bioinform. 9, 299–306.

Lewis, L.A., McCourt, R.M., 2004. Green algae and the origin of land plants. Am. J. Bot. 91, 1535–1556.

Maddison, W.P., Maddison, D.R., 2006. Mesquite: a Modular System for Evolutionary Analysis. Version 1.1. <http://mesquiteproject.org>.

Martín-González, A., Wierzchos, J., Gutiérrez, J.C., Alonso, J., Ascoso, C., 2008. Morphological stasis of protists in Lower Cretaceous amber. Protist 159, 251–257.

Mason-Gamer, R., Kellogg, E., 1996. Testing for phylogenetic conflict among molecular data sets in the tribe *Triticeae* (Gramineae). Syst. Biol. 45, 524–545.

Meindl, U., 1993. *Micrasterias* cells as a model system for research on morphogenesis. Microbiol. Rev. 57, 415–433.

Neustupa, J., Škaloud, P., 2007. Geometric morphometrics and qualitative patterns in the morphological variation of five species of *Micrasterias* (Zygnemophyceae, Viridiplantae). Preslia 79, 401–417.
Neustupa, J., Šťastný, J., Hodač, L., 2008. Temperature-related phenotypic plasticity in the green microalga *Micrasterias rotata*. Aquat. Microb. Ecol. 51, 77–86.
Neustupa, J., Černá, K., Šťastný, J., 2009a. Diversity and morphological disparity of desmid assemblages in Central European peatlands. Hydrobiologia 630, 243–256.
Neustupa, J., Němcová, Y., Eliáš, M., Škaloud, P., 2009b. *Kalinella bambusicola* gen. Et sp. nov. (Trebouxiophyceae, Chlorophyta), a novel coccoid *Chlorella*-like subaerial alga from Southeast Asia. Phycol. Res. 57, 159–169.
Neustupa, J., Škaloud, P., Šťastný, J., 2010. The molecular phylogenetic and geometric morphometric evaluation of *Micrasterias crux-melitensis*/*M. Radians* species complex. J. Phycol. 46, 703–714.
Pagel, M., Meade, A., 2006. Bayesian analysis of correlated evolution of discrete characters by Reversible-Jump Markov Chain Monte Carlo. Am. Nat. 167, 808–825.
Paradis, E., Claude, J., Strimmer, K., 2004. APE: analyses of phylogenetics and evolution in R language. Bioinformatics 20, 289–290.
Pickett-Heaps, J.D., 1975. Green Algae: Structure, Reproduction, and Evolution in Selected Genera. Sinauer Associates, Sunderland, MA.
Posada, D., Crandall, K.A., 1998. Modeltest: testing the model of DNA substitution. Bioinformatics 14, 817–818.
Prescott, G.W., Croasdale, H.T., Vinyard, W.C., 1977. A Synopsis of North American Desmids, Part II. Desmidiaceae: Placodermae, Section 2. University of Nebraska Press, Lincoln.
Ralfs, J., 1848. British Desmidieae. Reeve, Benham, and Reeve, London.
Rieseberg, L.H., Willis, J.H., 2007. Plant speciation. Science 317, 910–914.
Ronquist, F., Huelsenbeck, J.P., 2003. MRBAYES 3: Bayesian phylogenetic inference under mixed models. Bioinformatics 19, 1572–1574.
Růžička, J., 1981. Die Desmidiaceen Mitteleuropas. Band 1(2). Lieferung. E. Schweizerbart'sche Verlagsbuchhandlung, Stuttgart.
Schmidt, H.A., Strimmer, K., Vingron, M., von Haeseler, A., 2002. TREE-PUZZLE: maximum likelihood phylogenetic analysis using quartets and parallel computing. Bioinformatics 18, 502–504.
Schöniger, M., von Haeseler, A., 1994. A stochastic model for the evolution of autocorrelated DNA sequences. Mol. Phylogenet. Evol. 3, 240–247.
Skaloud, P., Peksa, O., 2010. Evolutionary inferences based on ITS rDNA and actin sequences reveal extensive diversity of the common lichen alga *Asterochloris* (Trebouxiophyceae, Chlorophyta). Mol. Phylogenet. Evol. 54, 36–46.
Skuja, H., 1964. Grundzüge der Algenflora und Algenvegetation der Fjeldgegend um Abisko in Schwed.-Lappland. Nova Acta Reg. Soc. Sci. Upsal., Ser. IV 18, 1–465.
Sormus, L., Bicudo, C.E.M., 1974. Polymorphism in the desmid *Micrasterias pinnatifida* and its taxonomic implications. J. Phycol. 10, 274–279.
Strimmer, K., von Haeseler, A., 1997. Likelihood-mapping: a simple method to visualize phylogenetic content of a sequence alignment. Proc. Natl. Acad. Sci. USA 94, 6815–6819.
Swofford, D.L., 2002. PAUP*. Phylogenetic Analysis Using Parsimony (*and Other Methods). Version 4. Sinauer Associates, Sunderland, Massachusetts.
Šťastný, J., 2009. The desmids of the Swamp Nature Reserve (North Bohemia, Czech Republic) and a small neighbouring bog: species composition and ecological condition of both sites. Fottea 9, 135–148.
Teiling, E., 1956. On the variation of *Micrasterias mahabuleshwarensis* f. *Wallichii*. Bot. Notiser 109, 260–274.
Turner, W.B., 1892. The fresh water algae (principally Desmidieae) of East India. Koning. Sv. Vet. Akad. Handl. 25, 1–187.
Tyler, P.A., 1970. Taxonomy of Australian freshwater algae. I. The genus *Micrasterias* in south-eastern Australia. Brit. Phycol. J. 5, 211–234.
Verbruggen, H., 2009. TreeGradients. <http://www.phycoweb.net>.
Verbruggen, H., Maggs, C.A., Saunders, G.W., Le Gall, L., Yoon, H.S., De Clerck, O., 2010. Data mining approach identifies research priorities and data requirements for resolving the red algal tree of life. BMC Evol. Biol. 10, 1–16.
Waris, H., 1950. Cytophysiological studies on *Micrasterias*. I. Nuclear and cell division. Physiol. Plant. 3, 1–16.
Waris, H., Kallio, P., 1964. Morphogenesis in *Micrasterias*. Adv. Morphog. 4, 45–80.
West, G.S., 1909. The algae of the Yan Yean Reservoir, Victoria: a biological and ecological study. J. Linn. Sot. Bot. 39, l–88.
West, W., 1889. The freshwater algae of Maine. J. Bot. 27, 205–207.
West, W., West, G.S., 1905. A Monograph of the British Desmidiaceae, vol. 2. Ray Society, London.
Zelditch, M.L., Swiderski, D.L., Sheets, D.H., Fink, W.L., 2004. Geometric Morphometrics for Biologists: a Primer. Elsevier Academic Press, London.

Supplementary Data 1. List of taxa used in the study, along with the obtained morphological data (number of terminal lobes, branching pattern of polar lobes, cell complexity, and cell length). The GenBank accession numbers for the SSU rDNA, *psa*A and *cox*III genes are also provided. Strain number abbreviations: ASW - Culture Collection of Algae, University of Vienna, nowadays deposited in the Culture Collection of Algae at the University of Cologne (CCAC); CAUP - Culture Collection of Algae, Charles University in Prague; NIES - Microbial Culture Collection, National Institute for Enviromental Studies, Onogawa; SAG - Culture Collection of Algae, Georg-August University Göttingen; SVCK - Sammlung von Conjugaten-Kulturen, University Hamburg.

Taxon name	Strain number	Morphological characteristics mapped on the phylogenetic tree				GenBank accession numbers		
		Number of terminal lobes per semicell	Branching pattern of polar lobes	Cell complexity	Cell length	SSU rDNA gene	*psa*A gene	*cox*III gene
Micrasterias americana Ehrenberg ex Ralfs	SVCK 290	4	1	1.59064	140	FR852595	FR852626	FR852666
Micrasterias anomala W.B. Turner	NIES 774	5	2	1.551227	209	-	FR852627	FR852667
Micrasterias apiculata Meneghini ex Ralfs	SVCK 247	8	2	1.426105	230	FR852596	FR852628	FR852668
Micrasterias brachyptera P. Lundell	SVCK 65	8	2	1.64677	205	FR852597	FR852629	FR852669
Micrasterias ceratofera Joshua	SAG 21.97	2	1	1.448164	131	FR852598	FR852630	FR852670
Micrasterias conferta P. Lundell	SVCK 110	8	2	1.623739	90	FR852600	FR852632	FR852672
Micrasterias crux-melitensis Ralfs	CAUP K602	4	1	1.845687	107	AM419206	FR852633	FR852673
Micrasterias crux-melitensis Ralfs	NIES 152	4	1	1.865042	113	FR852601	FR852634	FR852674
Micrasterias decemdentata (Nägeli) W.Archer	ASW 07023	2	1	1.334061	50	FR852602	FR852635	FR852675
Micrasterias denticulata Brébisson ex Ralfs	SVCK 230	15	2	1.932418	217	FR852603	FR852636	FR852676
Micrasterias fimbriata Ralfs	CAUP K608	6	2	1.962178	235	FR852604	FR852637	FR852677
Micrasterias foliacea Bailey ex Ralfs	NIES 777	7	2	2.052426	80	-	FR852638	FR852678
Micrasterias furcata C. Agardh ex Ralfs	CAUP K609	4	1	2.545707	153	FR852605	FR852639	FR852679
Micrasterias hardyi G.S. West	SVCK 249	2	1	2.143069	216	FR852606	FR852640	FR852680
Micrasterias jenneri Ralfs	SVCK 298	8	2	1.341453	157	FR852607	FR852641	FR852681
Micrasterias laticeps Nordstedt	SVCK 430	1	0	1.185784	150	FR852608	FR852642	FR852682
Micrasterias mahabuleshwarensis J. Hobson	SVCK 324	2	1	1.802018	160	FR852609	FR852643	FR852683
Micrasterias muricata Bailey ex Ralfs	SAG 157.80	2	1	1.58329	175	FR852610	FR852644	FR852684
Micrasterias novae-terrae (Cushman) Krieger	SAG 158.80	6	2	2.242455	124	FR852611	FR852645	FR852685
Micrasterias papillifera Brébisson ex Ralfs	CAUP K603	8	2	2.299155	130	AM419208	FR852646	FR852686
Micrasterias pinnatifida Ralfs	SVCK 411	1	0	1.220962	61	FR852612	FR852647	FR852687
Micrasterias ‚pusilla' G.C. Wallich	NIES 784	4	1	1.348246	60	FR852621	FR852658	FR852698
Micrasterias radians var. bogoriensis (Bernard) Krieger	SVCK 389	6	2	2.355276	102	FR852613	FR852648	FR852688
Micrasterias radians var. evoluta (W.B. Turner) Krieger	SVCK 518	4	1	1.999237	107	FR852614	FR852649	FR852689
Micrasterias radiosa Ralfs	SVCK 303	14	2	3.135475	175	FR852615	FR852650	FR852690
Micrasterias rotata Ralfs	CAUP K604	12	2	2.164567	260	AM419209	FR852651	FR852691
Micrasterias semiradiata Brébisson ex Kützing	CAUP K606	4	1	1.482767	96	AM419211	FR852659	FR852699
Micrasterias swainei W.N. Hastings	SVCK 138	10	2	3.142072	155	FR852616	FR852652	FR852692
Micrasterias tetraptera West et G.S. West	SVCK 195	8	2	2.056462	116	FR852617	FR852653	FR852693
Micrasterias thomasiana W. Archer	CAUP K605	16	2	2.45181	220	AM419210	FR852654	FR852694
Micrasterias torreyi Bailey ex Ralfs	SVCK 369	5	2	2.527322	443	FR852618	FR852655	FR852695
Micrasterias tropica Nordstedt	SVCK 368	1	0	1.132613	106	FR852619	FR852656	FR852696
Micrasterias truncata Ralfs	SVCK 412	2	1	1.278057	100	FR852620	FR852657	FR852697
Micrasterias zeylanica F.E.Fritsch	SVCK 291	2	1	1.169259	57	FR852599	FR852631	FR852671
Cosmarium ralfsii Brébisson ex Ralfs	SVCK 300	0	0	0.7989802	116	FR852622	FR852660	FR852700
Staurodesmus dickiei (Ralfs) Lillieroth	ASW 07056	0	0	0.75505	39	FR852623	FR852661	FR852701
Triploceras gracile Bailey	SAG 24.82	0	0	0.6973971	400	AJ428089	EF371259	EF371151
Triploceras gracile Bailey	SVCK 366	0	0	0.6973971	400	FR852624	FR852662	FR852702
Staurastrum lunatum Ralfs	SVCK 15	0	0	0.873074	37	AJ428106	FR852663	FR852703
Staurastrum maamense W. Archer	SVCK 377	0	0	0.771196	38	AJ829646	-	FR852704
Staurastrum majusculum F. Wolle	SVCK 330	0	0	1.373136	56	AJ829635	FR852664	FR852705
Hyalotheca mucosa Ralfs	SVCK 103	-	-	-	-	FR852625	FR852665	FR852706